ISSN No:-2456-2165

Porkchop Plot of a Direct Earth-Mercury Trajectory using Lambert's Problem

Gisa G S[1]
Assistant Professor
[1]Department of Aerospace Engineering, Alliance University, Bangalore

Hariprasad Thimmegowda[2]
Assistant Professor
[2]Department of Aerospace Engineering, Alliance University, Bangalore

Yadu Krishnan S[3]
Assistant Professor
[3]Department of Aerospace Engineering, Alliance University, Bangalore

Abstract:- Numerous space missions have minimal energy requirements, which are calculated and stated as rocket vehicle velocity requirements. This provides a quick opportunity for an impression of the ideal vehicle or an estimate of the payload capacity of a particular vehicle. As we move closer to the inner planets of the solar system, solar radiation's effects worsen and so do the energy requirements. This energy need can be reduced using flyby missions. A porkchop plot used in orbital mechanics displays contours of even characteristic energy based on numerous permutations of the date of launch and the date of arrival for a precise interplanetary voyage. The porkchop plot solutions, decide the endurance of a launch window for a particular spacecraft. In this study, the porkchop plots for the Earth-Mercury direct transfer are plotted by using the departure date, arrival date, and flight duration as fixed values in the orbital components of the solution, generally known as Lambert's problem. For this study, non – coplanar, non – circular orbits of the planets are considered. The patched conic method is used to create mission prospects. For the years 2021-2030, porkchop plots are produced. The simulation results utilizing Free flyer for this window are included.

***Keywords*:-** *Interplanetary Trajectories; Non-Hohmann Transfer; Lambert's Problem; Direct Trajectory.*

I. INTRODUCTION

Most interplanetary trajectory designs are based on the supposition that planetary orbits are circular, their orbital planes align by the plane of orbit of the Earth, and the transfer trajectory positioning in this ecliptic plane.

Reinforced understanding of low-thrust space courses' design is examined in [1], that is subjected to vagueness and instability. These are alternatively modelled as Gaussian additive method noise, and arbitrary faults in controlling the thrust, including the occurrence of an overlooked thrust issue. Intricate paths of the trajectories of a variety of bodies (such as spacecraft and comets), reflecting findings of twenty years in multipurpose flights are depicted in [2]. Most of the theoretical mathematics in this book [3], is followed by explanations of real-world applications that are used in tried-and-true software routines, which makes it unique. The book, for instance, has a collection of methods that experts and students can use to accurately calculate orbits on a computer.

The graphical data regarding possible Earth-Mars trajectories from 2026 to 2045 is given in [4]. The following opportunity contour maps were produced using the trajectory data produced by the patched conic interplanetary trajectory optimisation programme MIDAS. Initial strategy of Venus-bound supersonic missions and its pictorial data is provided in [5], along with many other launches and Venus's arrival parameters and present all launch opportunities from 1991 to 2005 in a launch date, and arrival date space.

Cianciolo et al., [6] had discussed about the improvement, implementation, furthermore outcomes of a pork chop map assessment about Mars Learning Test centre commission. Menzio et al., [7] performed a comprehensive investigation into the location and structure for single and multi-revolution trajectories.

Yuan, J et al., [8] had glanced into several topics, such as scheming the intermediate trajectory with a small thrust by simulated gravity arena technique and to perform transference in a system with 3 bodies, that either offer fresh approaches to solving well-known difficulties or address brand-new issues that haven't been thoroughly researched. [8] demonstrated how to make the pork chop plots of cost and cost sensitivity of interplanetary trips as a function of the mass of the payload, the maintenance needs of the destination orbit, and the engine-specific impulse.

George, L. E. et al., [9] had given mission designers and trajectory designers information about possible Earth-Mars and Mars-Earth trajectories from 2009 to 2024. These investigations were carried out in support of the below-described hypothetical human Mars mission scenario. MAnE-Mission Analysis Environment software package was used for its optimisation and to create all the trajectories and "porkchop plots".

ISSN No:-2456-2165

Giorgini, J. [10] had specified digital versions of technical publications written by JPL workers are stored in the JPL Open Repository (JOR), which will take the role of the JPL Technical Report Server (TRS) in 2023. The website [11] helps us generate the ephemeris data such as orbital elements of the target body, observer location, and time specification.

In this paper, non – coplanar, non – circular orbits of the planets are considered. Mission possibilities are created using the patched conic approach. This mission's design is based on Lambert's problem's solution.

II. METHODOLOGY

➢ *Non-Hohmann Interplanetary Trajectories*

All the planetary orbits are elliptical and are inclined with the ecliptic plane hence the transfer trajectories are non – coplanar [12].

The relative configuration of the transfer trajectory will not always be the same because of the eccentricity and inclination of the target planets about the Earth. The amount of time needed for the planet to return to the same location in its orbit is known as the synodic period. Because of this, computing these non-coplanar transfer trajectories is challenging.

A direct transfer non- coplanar trajectory can be determined as follows:

The departure time from the Earth t_D, and the arrival time to the target planet t_A are chosen. Then the flight duration can be determined as arrival time minus departure time ($t_A - t_D$). The heliocentric positions of the planet from where it departs and planet to which it arrives is determined by using planetary ephemerides.

The heliocentric transfer angle travelled by the spacecraft is given by:

$$\cos(\Delta\theta) = \frac{\bar{R_e} \cdot \bar{R}}{R_e\ R_t} \qquad [2.1.1]$$

C represents a chord that connects the Earth at leaving and the target planet on inception and is determined by:

$$c = R_{e_2} + R_{t_2} - 2R_e\ R_t \cos(\Delta\theta) \qquad [2.1.2]$$

Once the chord line has been established, solution of Lambert's question is solved for the provided flight period. This yields the orbital components of the transfer path. Following are the heliocentric velocities V_1 and V_2.

$$V_1 = \sqrt{\mu_s \left(\frac{2}{R_e} - \frac{1}{a}\right)} \qquad [2.1.3]$$

$$V_2 = \sqrt{\mu_s \left(\frac{2}{R_t} - \frac{1}{a}\right)} \qquad [2.1.4]$$

The formula for the flight path angle and the formulae for β_1 *and* β_2 are given by:

$$\gamma_1 = \frac{1}{2}(\beta_1 - \beta_2) \qquad [2.1.5]$$

$$\cos_{\beta_1} = \frac{R_e^2 - R_t^2 + c^2}{2cR_e};\ \cos_{\beta_2} = \frac{(2a - R_e)^2 - (2a - R_t)^2 + c^2}{2c\,(2a - R_e)}; \qquad [2.1.6]$$

Once the flight path angles are known, the semi latus rectum can be determined as,

$$p = \frac{(R_e V_1 \cos\gamma_1)^2}{\mu_s} \qquad [2.1.7]$$

The eccentricity is obtained by:

$$e = \sqrt{1 - \frac{p}{a}} \qquad [2.1.8]$$

The true anomaly with sun as the centre, on departing from the Earth is given as:

$$\theta_1 = \arccos\left\{\frac{1}{e}\left(\frac{p}{R_e} - 1\right)\right\} \qquad [2.1.9]$$

Therefore, true anomaly with sun at centre at the time of arrival exists to be:

$$\theta_2 = \theta_1 + \Delta\theta \qquad [2.1.10]$$

The transferal path's incline compared with the plane of earth's orbit is:

$$\cos i = \overline{e_w}.\overline{e_z} \quad [2.1.11]$$

Where e_w denotes unit vector perpendicular toward plane of orbit given as follows:

$$\overline{e_w} = \frac{\overline{R_e} \times \overline{R_t}}{R_e R_t \sin \Delta\theta} \quad [2.1.12]$$

Now the hyperbolic surplus velocities at the leaving and on onset are attained as tails:

$$V_{\infty\, dep} = V_1 - V_e \quad [2.1.13]$$

$$V_{\infty\, arr} = V_2 - V_e \quad [2.1.14]$$

Where V_1 and V_2 are the spacecraft's departure and arrival velocities.

- *The Lambert's Problem*

According to celestial mechanics, it calculates a trajectory using 2 radius vectors and the flight time.

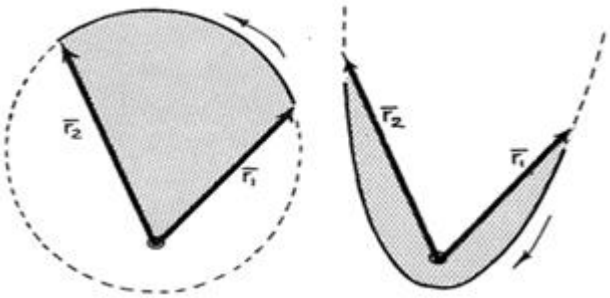

Fig 1 Lambert's Problem

Find $v_1 and\ v_2$, given the radius vectors, r_1, r_2, and the motion flow needs to be identified.

By determining this, it is decided whether the spacecraft must obtain a short way ($\Delta v < \Pi$ radians), or a long way ($\Delta v > \Pi$ radians) while travelling from $r_1 to\ r_2$. Out of the endless possibilities of an orbit passing through$\overline{r_1}\ and\ \overline{r_2}$, only 2 are possessing a required flight time, wherein both take apparent path of motion. $\overline{r_1}, and\ \overline{r_2}$ exclusively specify the intermediate orbit's plane. $\Delta v = \pi$ characterizes collinear vectors in reverse course. It is impossible to $v_1 and\ v_2$ for such flight path. $\Delta v = 0$ or 2π, depicts a degenerate conic, that gives an exclusive solution for v_1, and v_2.

$\overline{r_1}, \overline{r_2}, \overline{v_1}\ and\ \overline{v_2}$ can be correlated by using the following relations:

Lambert's problem can be solved by deriving from f and g relation:

$$r_2 = f r_1 + g v_1 \quad [2.2.1]$$

$$v_2 = f.r_1 + g.v_1 \quad [2.2.2]$$

And

$$f = 1 - \frac{\mu r_2}{p}(1 - \cos\Delta v) \quad [2.2.3]$$

$$g = \frac{r_1 r_2 \sin\varphi}{\sqrt{\mu p}} = -\sqrt{\frac{a^3}{\mu}}\ (\Delta E - \sin\Delta E) \quad [2.2.4]$$

$$\dot{f} = \sqrt{\frac{\mu}{p}}\tan\frac{\Delta v}{2}\left(\frac{1-\cos\Delta v}{p} - \frac{1}{r_1} - \frac{1}{r_2}\right) = \frac{-\sqrt{\mu a}}{r_1 r_2}\sin\Delta E \quad [2.2.5]$$

$$\dot{g} = 1 - \frac{r_1}{p}(1 - \cos\Delta v) = 1 - \frac{a}{r_2}(1 - \cos\Delta v) \quad [2.2.6]$$

$$v_1 = \frac{r_1 - f r_1}{g} \quad [2.2.7]$$

[2.2.2] and [2.2.7] give $v_1 and\ v_2$ and r_1 and r_2. Lambert's problem solution is thus achieved by assessing f, g, $\dot{f}, \dot{g}$.

$r_1, r_2, \Delta v, \Delta t, p, a, and\ \Delta E$ from [2.2.3], [2.2.4] and [2.2.5] give initial 4 known variables and later three equations in three unknowns.

- Firstly, out of p, a, or ΔE, we must guess a value for one of them, openly or implicitly by checking if any other transfer-related characteristics that were valid, additionally defined p, a, or E.
- Calculate the next two nonentities via [2.2.2] and [2.2.3].
- Resolve equation [2.2.4] instead of t and confirm the value obtained alongside the assumed time-of-flight.
- If calculated and provided values do not agree, change each variable's trial value, and continue the process until they do.
- Final phase determines how quickly the solution is attained.

➢ *Lambert's Problem Resolution*

By proceeding Lambert's problem answer, f and g are stated through 3 individual equations in 3 unknowns, p, a, and ΔE.

$$f = 1 - \frac{r_2}{p}(1 - cos\Delta v) = 1 - \frac{x^2}{r_1}c \quad [2.3.1]$$

$$g = \frac{r_1 r_2 sin\Delta v}{\sqrt{\mu p}} = t - \frac{x^3}{\sqrt{\mu}}\,S \quad [2.3.2]$$

$$\dot{f} = \sqrt{\frac{\mu}{p}}\frac{1-cos\Delta v}{sin\Delta v}\left(\frac{1-cos\Delta v}{p}\frac{1}{r_1} - \frac{1}{r_2}\right) = \frac{-\sqrt{\mu}}{r_1 r_2} * (1 - zS) \quad [2.3.3]$$

$$\dot{g} = 1 - \frac{r_1}{p}(1\text{-}cos\Delta v) = 1 - \frac{x^2}{r_2}\,C \quad [2.3.4]$$

x is obtained as follows:

$$x = \sqrt{\frac{r_1 r_2 (1 - cos\Delta v)}{pC}} \quad [2.3.5]$$

Substituting for x in equation [1.4.10] and cancelling $\frac{\sqrt{\mu}}{p}$ from both sides, yields

$$\frac{1-cos\Delta v}{sin\Delta v}\left(\frac{1-cos\Delta v}{p}\frac{1}{r_1} - \frac{1}{r_2}\right) = \sqrt{\frac{1-\Delta v}{r_1 r_2}}\frac{(1-zS)}{\sqrt{C}} \quad [2.3.6]$$

We define a constant A,

$$A = \frac{\sqrt{r_1 r_2 sin\Delta v}}{\sqrt{1 - cos\Delta v}} \quad [2.3.7]$$

$$Y = r_1 + r_2\frac{(1-zS)}{\sqrt{C}} \quad [2.3.8]$$

$$x = \sqrt{\frac{Y}{C}} \quad [2.3.9]$$

$$\sqrt{\mu t} = x^3 S + A\sqrt{Y} \quad [2.3.10]$$

After introducing A, $f, g,$ and $\dot{g}$ formulas in [2.3.1], [2.3.2], and [2.3.4] are simplified as:

$$f = 1 - \frac{Y}{r_1} \quad [2.3.11]$$

$$g = A\sqrt{\frac{Y}{\mu}} \quad [2.3.12]$$

ISSN No:-2456-2165

$$\dot{g} = 1 - \frac{Y}{r_2} \quad [2.3.13]$$

Since $r_2 = fr_1 + gv_1$,we can compute v_1 from

$$v_1 = \frac{r_2 - fr_1}{g} \quad [2.3.14]$$

The velocity v_2 may be expressed as

$$v_2 = \dot{f}r_1 + \dot{g}v_1 \quad [2.3.15]$$

Substituting for v_1 from eqn [1.4.21] and using the identity fg. -$\dot{f}g$=1, the last equation thus simplifies further simplifies to:

$$v_2 = \frac{\dot{g}r_2 - r_1}{g} \quad [2.3.16]$$

- *Procedure to resolve Lambert's problem via universal variables follows as below:*

- ✓ Evaluate the constant, A, with r_1, r_2 plus path of motion using [2.3.7]
- ✓ z =ΔE^2 and -z =ΔF^2. So, assume a value of z, that is equivalent to guessing on the eccentric anomaly change. z varies from minus values to $2\pi^2$. z > $2\pi^2$ corresponds to ΔE that is greater than 2π. Only when the satellite crosses from r_1 to r_2 does this occur.
- ✓ Use [2.3.10] and [2.3.11] to estimate S and C functions for the assumed z.
- ✓ Calculate Y using [2.3.10].
- ✓ Find out x from equation [2.3.9].
- ✓ The assumed z is verified by calculating t from [2.3.12]. This is compared with the required flight time. If the 2 values are not equal, assume a different value for z and continue the process until the target t is reached.
- ✓ When the methods converge to the result, assess f, g, and $\dot{g}$ using [2.3.11], [2.3.12], [2.3.13], [2.3.14], [2.3.15], and [2.3.16].

III. RESULTS AND DISCUSSIONS

➢ *Pork Chop Plots*

For a wide range of flight periods, many Lambert problems are solved from a fixed R_E that is, the position of the satellite while leaving the Earth. The outcome of this flight-time is shown in Figure 1, illustrating the two ideal transferals that reduce launching energy for specific departing dates. The best heliocentric transfers can be determined by varying the Earth departure and the flight duration. The flight duration is equal to $t_A - t_D$. Thus, for a variety of n different departure dates and m flight periods, a great deal of Lambert issues can be resolved. The total ideal heliocentric transfer that reduces launch energy C3 is identified by simply sorting the n m matrix of Lambert-problem solutions for an optimum date for departure and time of flight. To see the design space for the interstellar course, contoured graphs of the n m Lambert-problem solutions are helpful.

Figure 2's every line of contour illustrates C3 helium-centred transference for each line. This displays an ensemble of the short-way & long-way transfers, two different helium-centred paths. The ideal transfer that reduces C3 is in the middle of each set of curves. Amid Type 1 and Type 2 transfers, there is a sharp "ridge" denoting the area for a 180-degree transfer angle and the resulting C3 is remarkably considerable. The plot in Figure 2 is referred to as a pork-chop plot, employed to examine the launching window or the impact that variations in the departure date have on the launch energies and/or flight duration.

ISSN No:-2456-2165

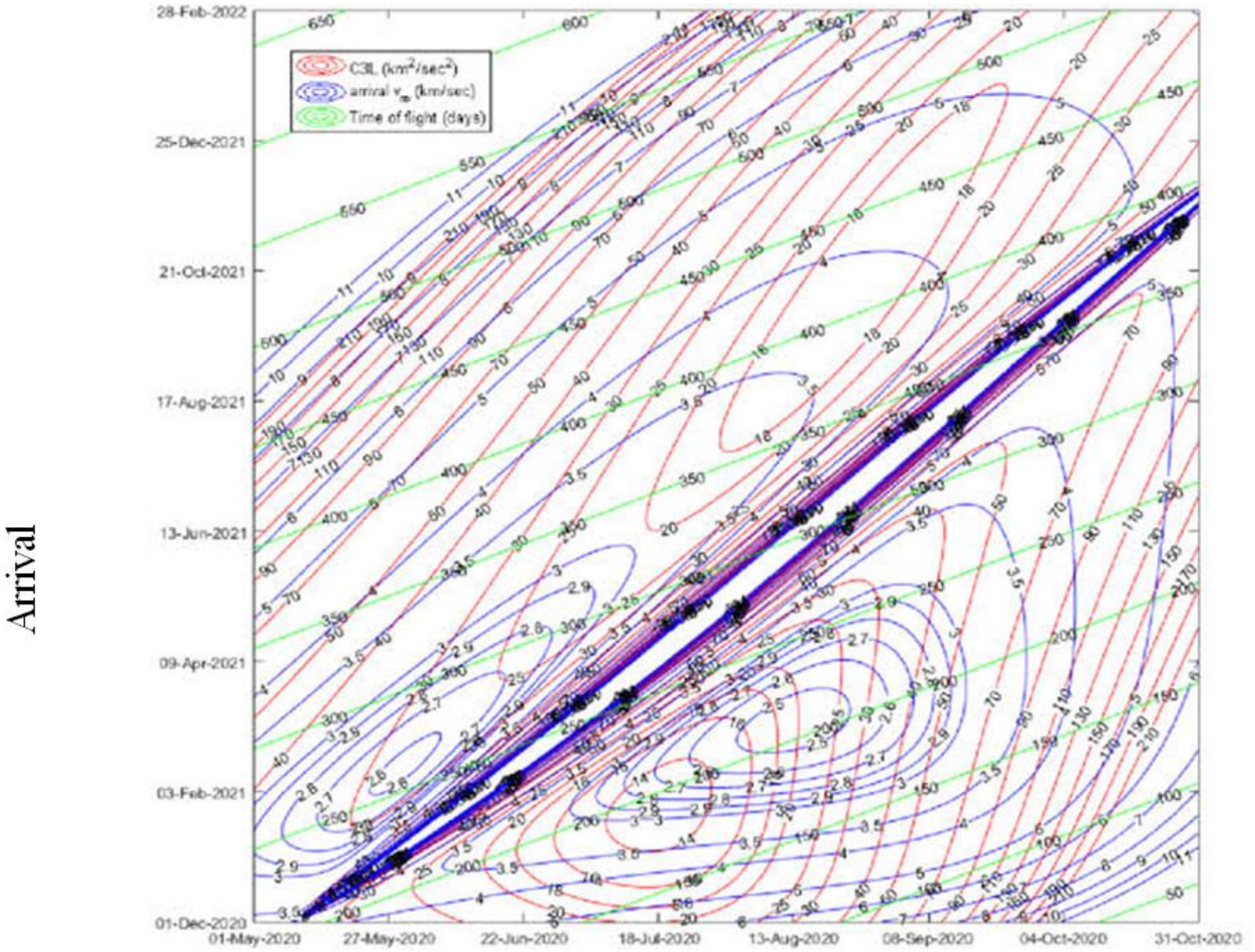

Fig 2 Porkchop Plot

```
>>import astropy.units as u

>>from poliastro.plotting.porkchop import porkchop
>>from poliastro.bodies import Earth, Mercury
>>from poliastro.util import time_range

>>launch_span = time_range("2021-01-01", end="2030-12-31")
>>arrival_span = time_range("2021-01-01", end="2030-12-31")
porkchop_plot = PorkchopPlotter(Earth, Mercury, launch_span, arrival_span)
dv_dpt, dv_arr, c3dpt, c3arr, tof = porkchop_plot.porkchop()
```

Fig 3 Python Code for the Pork Chop Plot

Table 1 provides a list of the possible direct missions between Mercury and Earth. Three minimum energy direct transfer chances between Earth and Mercury are shown in the table. The calculation timeframe for each mission opportunity is 2021 to 2030. The hyperbolic excess speeds of the launch window range from 17 km/s to 20 km/s. The year 2023 has the longest launch window with a 134-day flight, and the next year, 2030, offers a 128-day launch window. It is noted that 2026 will have the bare minimum launch window. Figure 3 depicts the departure excess velocity's pork chop plot for the years 2021 to 2022. The image also illustrates the little launch window with the best chance for using the least amount of energy. Figure 4 depicts the departure excess velocity's pork chop plot for the years 2021 to 2030. Figure 5 depicts the arrival excess velocity's pork chop plot for the years 2021 to 2030.

ISSN No:-2456-2165

Table 1 Total Hyperbolic Excess Speeds for Earth – Mercury direct transfer 2021-2030

Date of Launch	Date of Arrival	Flight duration (Days)	Excess velocity at departure (V□) dep (km/s)	Excess velocity on arrival (V□) arr (km/s)	Total hyperbolic excess speeds (km/s)
05/11/2021	**20/02/2022**	108	5.7372	11.71342	17.45062
15/10/2022	**06/02/2023**	114	6.6537	12.724	19.3777
10/05/2023	**21/09/2023**	134	11.9389	8.0739	20.01
10/05/2024	**04/09/2024**	117	10.4392	8.0994	18.5386
12/05/2025	**21/08/2025**	101	9.3672	8.0306	17.3978
06/05/2026	**03/08/2026**	90	9.569	8.3327	17.9017
06/11/2027	**01/03/2028**	116	6.6512	11.9158	18.567
26/10/2028	**15/02/2029**	112	6.6171	12.3473	18.9644
06/10/2029	**29/01/2030**	116	6.7884	12.9124	19.7008
09/05/2030	**14/09/2030**	128	11.3819	8.0105	19.3924

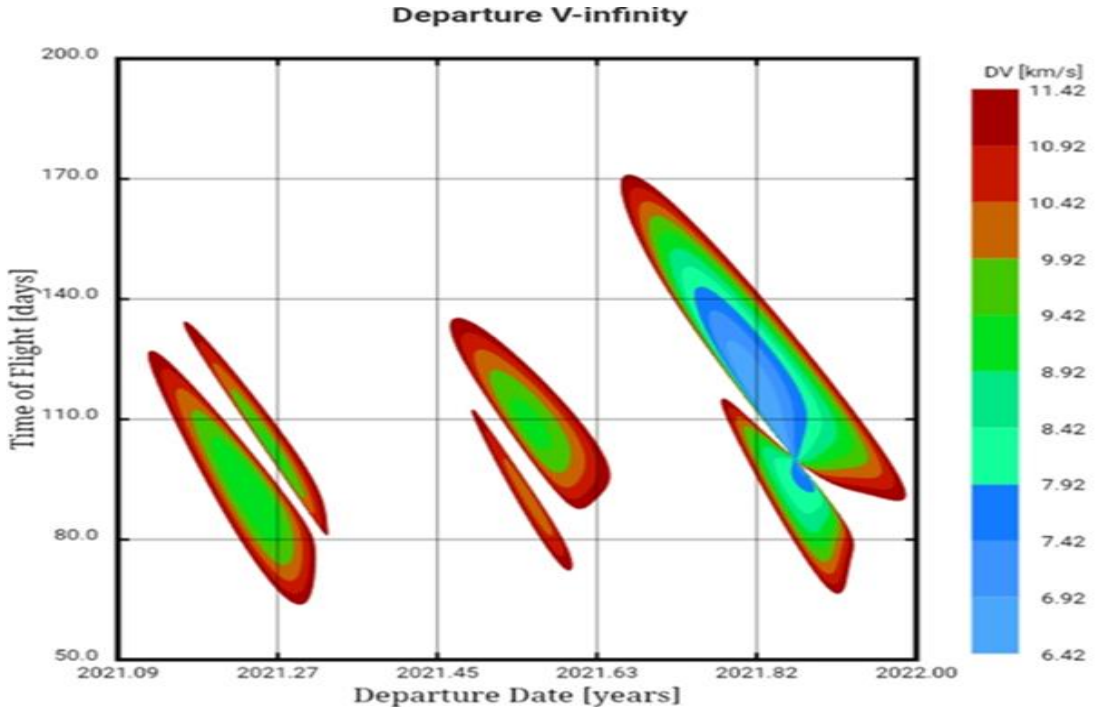

Fig 3 Pork Chop Graphic Shows the Earth-to-Mercury Direct Transfer's Departure Excess Velocity (2021- 2022)

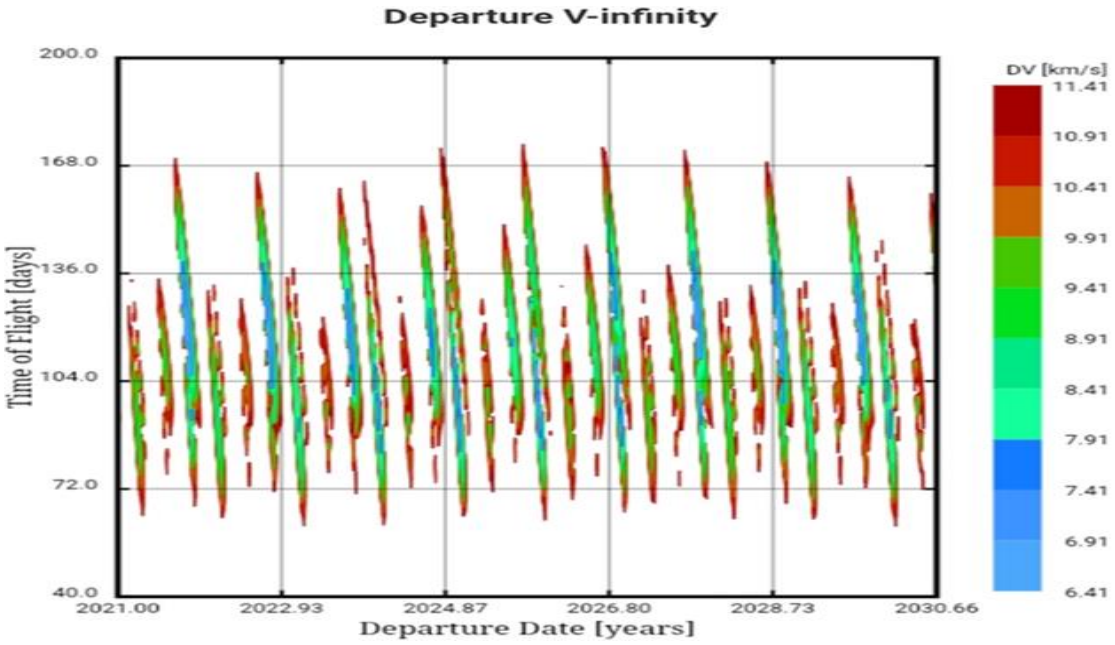

Fig 4 Pork Chop Plot of Departure Excess Velocity for Earth- Mercury Direct Transfer (2021- 2030)

ISSN No:-2456-2165

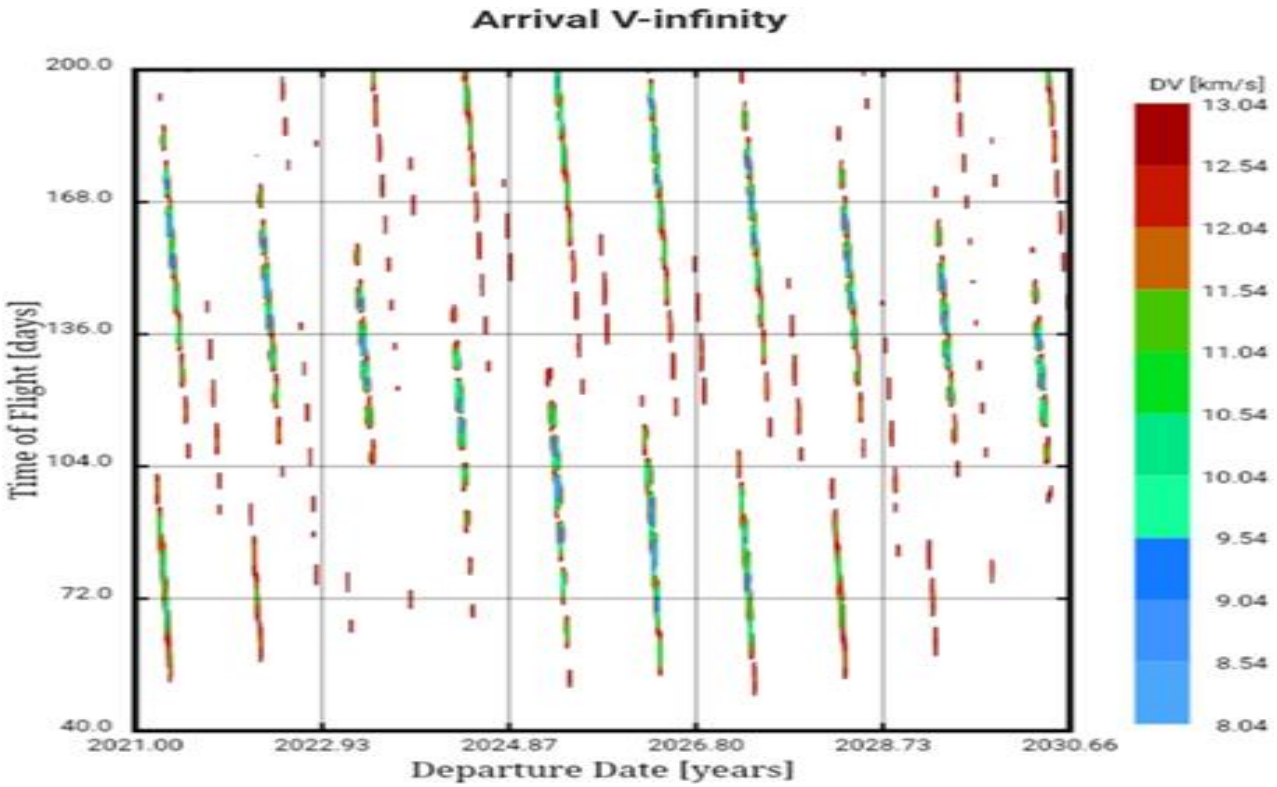

Fig 5 Pork Chop Plot of Arrival Excess Velocity for Earth- Mercury Direct Transfer (2021-2030)

➢ *Simulation Results using Free Flyer*

The Free flyer results for the following launch windows are obtained. These results prove the accuracy of the launch windows obtained analytically through the Lambert's problem for a variety of flight duration. It is verified that the minimum launch window is possible in the year 2026.

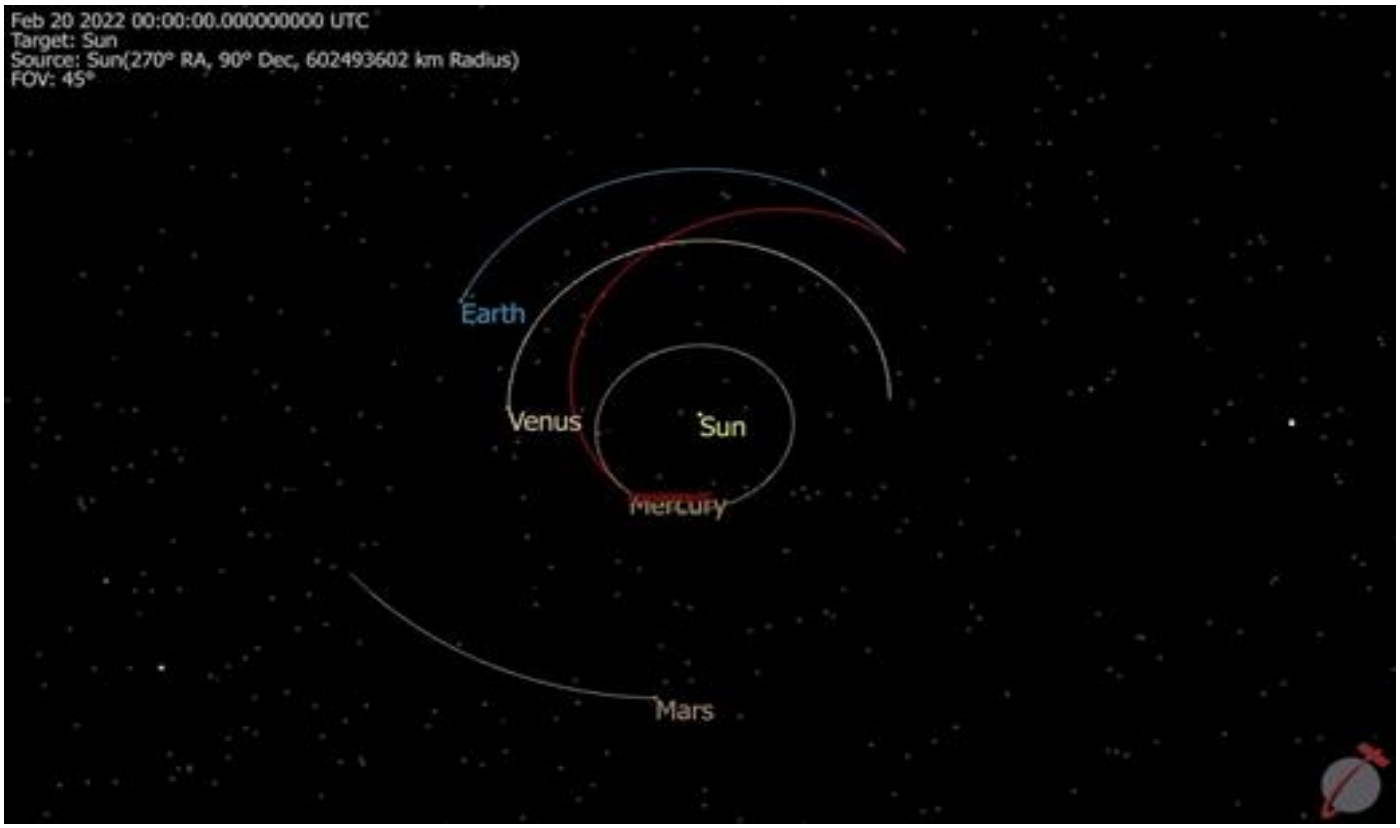

Fig 6 Earth – Mercury direct transfer for the launch window 05/11/2021 – 20/02/2022

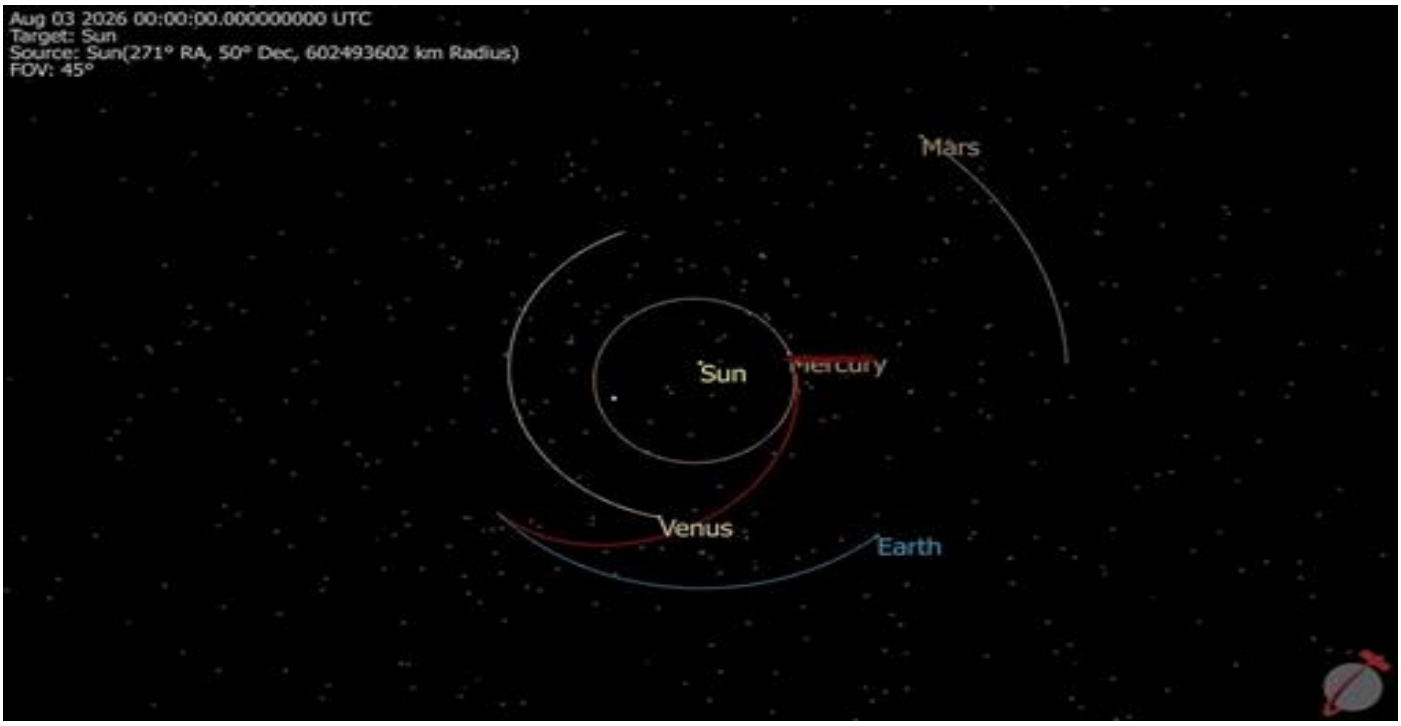

Fig 7 Earth – Mercury direct transfer for the launch window 06/05/2026 – 03/08/2026

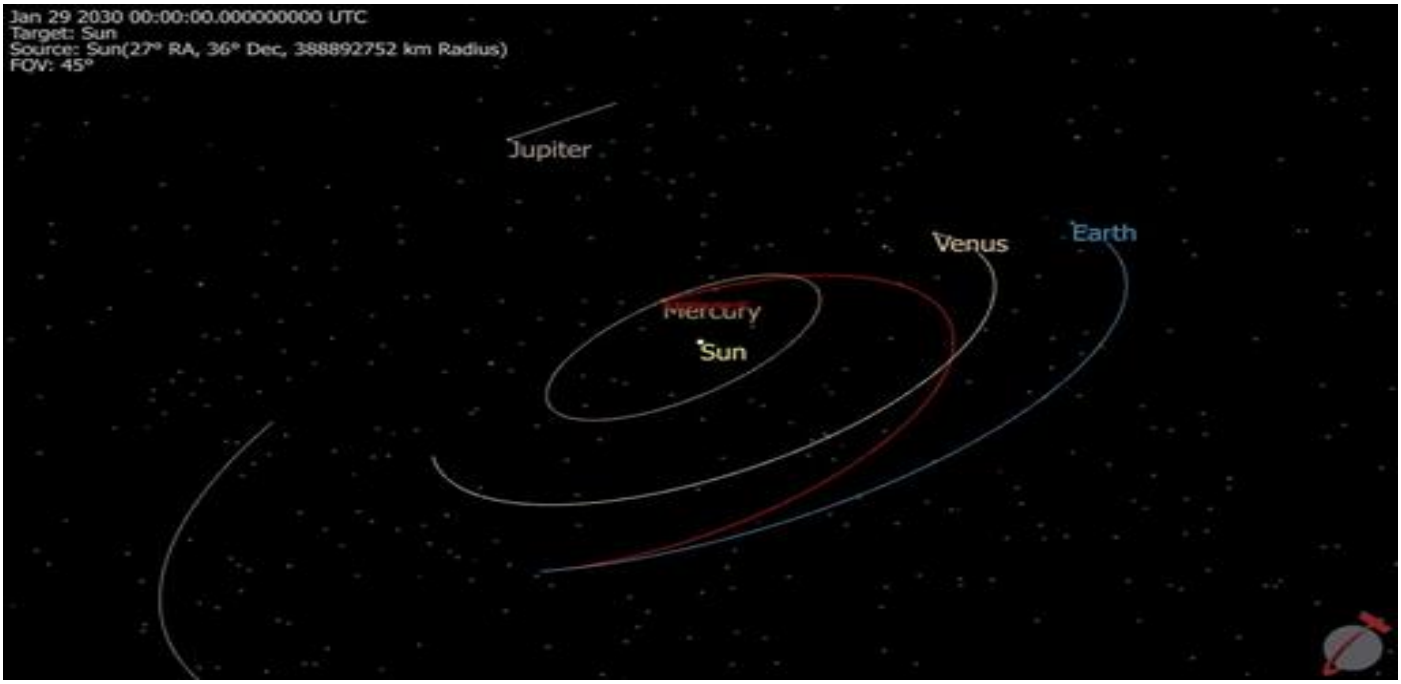

Fig 8 Earth – Mercury direct transfer for the launch window 06/10/2029 – 29/01/2030

IV. CONCLUSION

For a range of flight periods, multiple Lambert problems are solved from a given Earth-departure position vector, R_E. Each mission opportunity's computation window ranges from 2021 through 2030. By adjusting the Earth departure and flight time, the optimal heliocentric transfers are obtained. Pork-chop plots are used to investigate the effects of departure date variations on launch energies and/or flight duration. Pork chop plots for departure excess velocity for the years 2021–2023 are obtained, providing limited window for launch. For the years 2021–2030, pork chop plots for the departure excess velocity and arrival excess velocity are derived, giving a wide window for launch. It is observed that with a 134-day flight, the year 2023 offers the longest launch window, and the following year, 2030, has a 128-day window. For the launch windows, the simulation results are added using Free Flyer and the bare minimum launch window in the year 2026 is verified.

➢ *Nomenclature*

Table 2 Nomenclature

t_D	**Departure time from Earth**	**e**	**Eccentricity**
t_A	Arrival time to target planet (Mercury)	θ_1	True anomaly with sun as the centre, on departing from the Earth
$\Delta\theta$	Heliocentric transfer angle travelled by the spacecraft	θ_2	Heliocentric true anomaly on arrival
c	Chord that connects the Earth at leaving and the target planet on inception	i	Transferal path's incline
γ	Flight path angle	$V_{\infty\ dep}$	hyperbolic surplus velocity at the leaving
p	Semi latus rectum	$V_{\infty\ arr}$	Hyperbolic excess velocity on arrival
μ_s	Sun's gravitational constant	a	Semi-major axis

REFERENCES

[1]. Peralta, F., & Flanagan, S. (1995). Cassini interplanetary trajectory design. Control Engineering Practice, 3(11), 1603-1610.
[2]. Labunsky, A.V., Papkov, O.V. & Sukhanov, K.G., 1998. Multiple gravity assist interplanetary trajectories, Amsterdam: Gordon and Breach Science Publishers.
[3]. Vallado, D. And McClain, W., 2013. Fundamentals of astrodynamics and applications. 4th ed. Hawthorne (California): Microcosm Press
[4]. Burke, L. M., Falck, R. D., & McGuire, M. L. (2010). Interplanetary mission design handbook: Earth-to-mars mission opportunities 2026 to 2045 (No. NASA/TM-2010-216764).
[5]. Sergeyevsky, A.B. et al., 1983. Interplanetary mission design handbook, Pasadena, CA: National Aeronautics and Space Administration, Jet Propulsion Laboratory, California Institute of Technology.
[6]. Cianciolo, A. D., Powell, R., & Lockwood, M. K. (2006, March). Mars Science Laboratory launch-arrival space study: a pork chop plot analysis. In 2006 IEEE Aerospace Conference (pp. 10-pp). IEEE.
[7]. Menzio, D., & Colombo, C. (2018). An analysis of the pork-chop plot for direct and multi-revolution flyby missions. ADVANCES IN THE ASTRONAUTICAL SCIENCES, 165, 1739-1753.
[8]. Yuan, J., Cheng, Y., Feng, J., & Sun, C. (2019). Low Energy Flight: Orbital Dynamics and Mission Trajectory Design. Springer Singapore.
[9]. George, L. E., & Kos, L. D. (1998). Interplanetary mission design handbook: Earth-to-Mars mission opportunities and Mars-to-Earth return opportunities 2009-2024 (No. M-881).
[10]. Giorgini, J. (2020). JPL horizons overview and future plans.
[11]. Anon, HORIZONS Web-Interface, NASA. Available at:https://ssd.jpl.nasa.gov/horizons.cgi#results [Accessed June 11, 2021].
[12]. Curtis, H. D. (2020). Orbital Mechanics for Engineering Students: Revised Reprint. Butterworth-Heinemann.